Timo Bartsch, Christopher Benndorf, Hellmut Eckert, Matthias Eul and Rainer Pöttgen*

La₃Cu₄P₄O₂ and La₅Cu₄P₄O₄Cl₂: synthesis, structure and ³¹P solid state NMR spectroscopy

DOI 10.1515/znb-2015-0181 Received November 2, 2015; accepted November 18, 2015

Abstract: The phosphide oxides La₂Cu₄P₄O₂ and La₅Cu₄ P.O.Cl. were synthesized from lanthanum, copper(I) oxide, red phosphorus, and lanthanum(III) chloride through a ceramic technique. Single crystals can be grown in a NaCl/KCl flux. Both structures were refined from single crystal X-ray diffractometer data: I4/mmm, a = 403.89(4), c = 2681.7(3) pm, wR2 = 0.0660, 269 F^2 values, 19 variables for La₂Cu₄P₄O₅ and a = 407.52(5), c =4056.8(7) pm, wR2 = 0.0905, 426 F² values, 27 variables for La_cCu_cP_cO_cCl₃. Refinement of the occupancy parameters revealed full occupancy for the oxygen sites in both compounds. The structures are composed of cationic (La₂O₂)²⁺ layers and covalently bonded (Cu,P,)5- polyanionic layers with metallic characteristics, and an additional La3+ between two adjacent (Cu,P,)5- layers. The structure of La_sCu_aP_aO_aCl₃ comprises two additional LaOCl slabs per unit cell. Temperature-dependent magnetic susceptibility studies revealed Pauli paramagnetism. The phosphide substructure of La₃Cu₄P₄O₅ was studied by ³¹P solid state NMR spectroscopy. By using a suitable dipolar re-coupling approach the two distinct resonances belonging to the P₂⁴⁻ and the P3- units could be identified.

Keywords: crystal structure; pnictide oxide; solid state NMR spectroscopy.

1 Introduction

The structural chemistry of pnictide oxides is mainly characterized by the large family of ZrCuSiAs type compounds

*Corresponding author: Rainer Pöttgen, Institut für Anorganische und Analytische Chemie, Universität Münster, Corrensstrasse 30, 48149 Münster, Germany, e-mail: pottgen@uni-muenster.de Timo Bartsch and Matthias Eul: Institut für Anorganische und Analytische Chemie, Universität Münster, Corrensstrasse 30, 48149 Münster, Germany

Christopher Benndorf and Hellmut Eckert: Institut für Physikalische Chemie, Universität Münster, Corrensstrasse 30, 48149 Münster, Germany and Institute of Physics in Sao Carlos, University of Sao Paulo, Sao Carlos, SP 13560-970, Brazil

with the general formula *RETPnO* (RE = rare earth element, T = divalent transition metal cation, $Pn = P^{3-}$, As^{3-} , Sb^{3-}). These compounds have layer-like structures with an AB stacking of (REO)+ cationic and (TPn)- anionic layers [1–4]. Partial substitution of the oxygen site by fluorine can induce superconductivity. The so far highest transition temperature of 55 K was observed for $SmFeAsO_{1-x}F_x$ [5]. Complete fluorine occupancy within the tetrahedra is only possible with a lower-valent cation, e.g. in BaMnPF [6] or SrFeAsF ($\equiv (SrF)^+(FeAs)^-$) [7]. Such fluorine-centered layers also occur in $(SrF)_2Ti_2Pn_2O$ (Pn = As, Sb) [8] and $(SrF)_2Fe_2OQ_2$ (Q = S, Se) [9].

An entirely new slab in the family of pnictide oxides was observed in the structure of $\text{La}_5\text{Cu}_4\text{As}_4\text{O}_4\text{Cl}_2$ [10]. This phase was first obtained during systematic salt flux syntheses of samples in the La-Cu-As-O system. In contrast to many other synthesis attempts, the alkali halide flux was not inert and reacted as a so-called reactive flux [11], delivering the chloride anions for formation of $\text{La}_5\text{Cu}_4\text{As}_4\text{O}_4\text{Cl}_2$. The targeted synthesis was then possible from lanthanum filings, arsenic powder, copper(I) oxide, and lanthanum oxychloride.

Parallel work in the corresponding phosphide system now led to single crystals of $La_5Cu_4P_4O_4Cl_2$. Its crystal structure and magnetic properties are reported herein. We have also reinvestigated the structure of $La_3Cu_4P_4O_2$ [12] on the basis of single crystal diffraction data and ³¹P solid state NMR spectroscopy.

2 Experimental

2.1 Synthesis

Starting materials for the syntheses of $\text{La}_3\text{Cu}_4\text{P}_4\text{O}_2$ and $\text{La}_5\text{Cu}_4\text{P}_4\text{O}_4\text{Cl}_2$ were rods of lanthanum (Smart Elements, >99.9%), copper(I) oxide (ABCR, >99%), red phosphorus (ABCR, >99.99%) and anhydrous lanthanum chloride (ChemPur, >99.9%). Lanthanum was employed as filings, which were prepared from the rods under dried (sodium wire) paraffin oil, subsequently washed with cyclohexane and stored under argon prior to synthesis. Argon was purified by means of titanium sponge (900 K),

silica gel, and molecular sieves. Anhydrous lanthanum chloride was used to prepare LaOCl – a suitable precursor for the synthesis of La_sCu₄P₄O₄Cl₂ - which could be obtained by calcination (973 K, 24 h according to LaCl₂ + $H_0O \rightarrow LaOCl + 2HCl$ with the water partial pressure in air) and was checked for purity by X-ray powder diffraction.

Polycrystalline samples of La₃Cu₄P₄O₅ and La₅Cu₄ P₂O₂Cl₃ were prepared by weighing filings of lanthanum, copper(I) oxide, phosphorus and LaOCl in the case of the quintenary compound in the ideal stoichiometric ratios of 3:2:4 and 3:2:4:2, respectively. Amounts of 0.5 g of these mixtures were carefully ground, cold pressed to pellets at ca. 100 bar and sealed in evacuated silica tubes. Synthesis was carried out in a resistance furnace. The first annealing sequence for La₂Cu₄P₄O₅ was 573 K for 12 h followed by 773 K for 72 h. In the case of La_eCu_eP_eO_eCl₂ the sequence was 773 K (24 h) and 1173 K (72 h). Annealing rates were 50 K h⁻¹, with cooling by shutting off the furnace. After regrinding the obtained samples, they were again pressed to pellets and sealed in evacuated silica tubes. For the La_cCu_cP_cO_cCl_a sample the pellet was additionally placed in an alumina crucible. The second annealing sequences were carried out at higher temperatures of 1173 K (120 h) for La₂Cu₄P₄O₃ and 1473 K (48 h) followed by 1373 K (120 h) for La_eCu_eP_eO_eCl_e. Cooling of the La_eCu_eP_eO_e sample was again by shutting off the furnace, whereas La₂Cu₄P₄O₄Cl₂ was quenched in iced water. Single phase La₂Cu₄P₄O₅ was obtained as a polycrystalline black powder. Single crystals for structure determination were obtained from a salt flux synthesis. Powder of La₂Cu₄P₄O₃ (200–300 mg) and an equimolar NaCl/KCl mixture (~1 g) were sealed in an evacuated silica tube, heated to 1223 K (72 h) and slowly cooled by a rate of 2 K/h to 773 K and finally to ambient temperature by shutting off the furnace. Suitable single crystals could be obtained after dissolving the flux in demineralised water. In contrast, the quenched tablet of La₂Cu₂P₂O₂Cl₂ showed black color with metallic luster and suitable single crystals could be separated from the crushed sample. Unfortunately, La_eCu_eP_eO_eCl_e could not be obtained phase pure. LaOCl was always observed as a minor impurity in the X-ray powder pattern. Additionally, ³¹P MAS NMR spectra (see below) revealed further phosphorus species, mainly from amorphous phosphate impurities.

2.2 X-ray diffraction

The polycrystalline La₃Cu₄P₄O₅ and La₅Cu₄P₄O₆Cl₅ samples were characterized through Guinier powder patterns (Enraf-Nonius camera, type FR 552); imaging plate

detector, Fujifilm BAS-1800, $CuK_{\alpha 1}$ radiation and α -quartz (a = 491.30, c = 540.46 pm) as an internal standard. Leastsquares refinements led to the tetragonal lattice parameters listed in Table 1. Correct indexing of the patterns was ensured through intensity calculations [13].

Irregularly shaped black single crystals of La_cCu_c P₄O₄Cl₃ were selected from the crushed annealed pellet. La₂Cu₂P₄O₃ crystals were separated from a salt flux. The crystals were glued to thin quartz fibers using bees wax and first studied on a Buerger camera (using white Mo radiation) to check their quality. Intensity data were collected at ambient temperature on a Stoe IPDS-II diffractometer (graphite monochromated MoK_{α} radiation, $\lambda = 71.073$ pm, oscillation mode) for La₅Cu₄P₄O₄Cl₂ and in the case of La₂Cu₄P₄O₅ on a four-circle diffractometer (Stoe StadiVari, μ -source, Mo K_{α} radiation, $\lambda = 71.073$ pm, oscillation mode) with an open Eulerian cradle setup equipped with a reverse-biased silicon diode array detector (Dectris Pilatus 100 K, resolution: 487 × 195 pixel, pixel size: $0.172 \times 0.172 \text{ mm}^2$). Numerical absorption corrections (along with scaling for the StadiVari data set) were applied to the data sets. Details about the data collections and the crystallographic parameters are summarized in Table 1.

Table 1: Crystal data and structure refinement results for La₂Cu₄P₄O₃ and $La_sCu_AP_AO_aCl_3$; space group I4/mmm, Z=2.

| Empirical formula | La ₃ Cu ₄ P ₄ O ₂ | La ₅ Cu ₄ P ₄ O ₄ Cl ₂ |
|---|---|---|
| Formula weight, g mol ⁻¹ | 826.8 | 1207.5 |
| <i>a</i> , pm | 403.89(4) | 407.52(5) |
| <i>c</i> , pm | 2681.7(3) | 4056.8(7) |
| V, nm³ | 0.4375 | 0.6737 |
| Calculated density, g cm ⁻³ | 6.28 | 5.95 |
| Absorption coefficient, mm ⁻¹ | 24.5 | 22.5 |
| Detector distance, mm | 40 | 80 |
| Exposure time | 67 s | 15 min |
| ω range; increment, deg | - | 0-180; 1.0 |
| Integr. param. A; B; EMS | 9.0; -8.5; 0.040 | 10.3; 1.3; 0.013 |
| <i>F</i> (000), e | 726 | 1054 |
| Crystal size, µm³ | $80\times15\times3$ | $45\times20\times10$ |
| Transm. ratio (max/min) | 0.93/0.62 | 0.80/0.54 |
| θ range, deg | 5-33 | 2-32 |
| Range in <i>hkl</i> | $\pm 6, \pm 6, \pm 38$ | $\pm 6, \pm 6, \pm 60$ |
| Total no. reflections | 1050 | 2232 |
| Independent reflections/ R_{int} | 269/0.0593 | 426/0.0564 |
| Reflections with $I > 3 \sigma(I)/R_{\sigma}$ | 131/0.0974 | 283/0.0484 |
| Data/parameters | 269/19 | 426/27 |
| Goodness-of-fit on F ² | 1.08 | 2.10 |
| $R1/wR2$ for $I > 3 \sigma(I)$ | 0.0355/0.0574 | 0.0442/0.0879 |
| R1/wR2 for all data | 0.0905/0.0660 | 0.0671/0.0905 |
| Extinction coefficient | 78(18) | 220(40) |
| Largest diff. peak/hole, e Å-3 | 1.54/-2.11 | 2.53/-3.01 |
| | | |

2.3 Structure refinements

Both data sets showed body-centred tetragonal lattices with high Laue symmetry and no further systematic extinctions. Space groups I4/mmm were found to be correct during the structure refinements in agreement with earlier studies on La₂Cu₄P₄O₅ [12] and the arsenide La₅Cu₄As₄O₆Cl₅ [10]. The starting atomic parameters were deduced using the charge-flipping algorithm of Superflip [14], and both structures were refined with anisotropic displacement parameters for all atoms with Jana2006 [15]. For better comparison with the literature data, in the final refinement cycles we transformed the positions to the setting given in [10] and [12]. Refinement of the occupancy parameters in a separate series of least-squares cycles revealed full occupancy for all sites within two standard deviations. The final difference Fourier syntheses revealed no residual peaks. The refined atomic positions, displacement parameters, and interatomic distances are given in Tables 2 and 3.

Further details of the crystal structure investigation may be obtained from Fachinformationszentrum Karlsruhe, 76344 Eggenstein-Leopoldshafen, Germany (fax: +49-7247-808-666; e-mail: crysdata@fiz-karlsruhe.de, http://www.fiz-karlsruhe.de/request_for_deposited_data.html) on quoting the deposition number CSD-430391 (La,Cu,P,O,) and CSD-430390 (La,Cu,P,O,Cl,).

2.4 EDX data

The irregularly shaped $La_3Cu_4P_4O_2$ and $La_5Cu_4P_4O_4Cl_2$ crystals studied on the diffractometers were semiquantitatively

analyzed by EDX using a Zeiss EVO® MA10 scanning electron microscope in variable pressure mode. LaF3, Cu, GaP, and KCl were used as standards. Except the oxygen content, the experimentally observed compositions were all within ± 3 at % close to the ideal ones. No impurity elements – especially chlorine in the case of La3Cu4P4O2 – were detected.

2.5 Physical property measurements

Magnetic susceptibility measurements of ${\rm La_5Cu_4P_4O_4Cl_2}$ were carried out on a Quantum Design Physical Property Measurement System (PPMS) using the VSM option. 31.643 mg of the powdered sample were packed in a polypropylene capsule and attached to the sample holder rod. Measurements were performed in the temperature range of 3–300 K with magnetic flux densities up to 80 kOe (1 kOe = 7.96×10^4 A m⁻¹).

2.6 31P solid state MAS NMR

 31 P solid state MAS NMR spectra of La $_3$ Cu $_4$ P $_4$ O $_2$ were recorded on a Bruker Avance III 300 MHz spectrometer ($B_0=7.05$ T) with spinning speeds of 28 and 30 kHz in conventional cylindrical ZrO $_2$ MAS rotors with 2.5 mm diameter at a resonance frequency of 121.442 MHz. The sample was ground and mixed with powdered quartz under dry cyclohexane to reduce the density and electrical conductivity. The experiments were carried out with

Table 2: Atomic coordinates with equivalent isotropic and anisotropic displacement parameters (pm²) of La₃Cu₄P₄O₂ and La₅Cu₄P₄O₄Cl₂. U_{eq} is defined as one third of the trace of the orthogonalized U_{ij} tensor. The site occupation factors (SOF) are given. $U_{12} = U_{13} = U_{23} = 0$.

| Atom | Wyckoff site | х | у | z | U ₁₁ | U ₂₂ | U ₃₃ | $oldsymbol{U}_{	ext{eq}}$ | SOF |
|--|--------------------------------|-----|-----|------------|------------------------|------------------------|------------------------|---------------------------|---------|
| La ₃ Cu ₄ P ₄ | 0, | | | | | | | | |
| La1 | 2 <i>a</i> | 0 | 0 | 0 | 136(7) | $U_{_{11}}$ | 220(13) | 164(6) | 1.03(2) |
| La2 | 4 <i>e</i> | 1/2 | 1/2 | 0.20275(7) | 173(6) | U_{11} | 213(9) | 186(4) | 1.02(2) |
| Cu | 8 <i>g</i> | 1/2 | 0 | 0.09436(9) | 200(11) | 200(11) | 213(13) | 204(7) | 0.97(2) |
| P1 | 4 <i>e</i> | 0 | 0 | 0.1397(3) | 137(18) | $U_{_{11}}$ | 270(50) | 183(18) | 0.98(3) |
| P2 | 4 <i>e</i> | 1/2 | 1/2 | 0.0424(3) | 180(20) | U_{11} | 160(30) | 175(14) | 1.04(4) |
| 0 | 4 <i>d</i> | 1/2 | 0 | 1/4 | 200(60) | U_{11} | 290(110) | 230(50) | 1.10(9) |
| La ₅ Cu ₄ P ₄ | 0 ₄ Cl ₂ | | | | | | | | |
| La1 | 4 <i>e</i> | 0 | 0 | 0.36646(4) | 99(5) | $U_{_{11}}$ | 132(8) | 110(3) | 1.02(2) |
| La2 | 4 <i>e</i> | 0 | 0 | 0.80609(4) | 108(5) | U_{11} | 128(7) | 115(3) | 1.03(2) |
| La3 | 2 <i>a</i> | 0 | 0 | 0 | 105(7) | U_{11} | 162(10) | 124(5) | 1.03(2) |
| Cu | 8 <i>g</i> | 0 | 1/2 | 0.43789(6) | 147(13) | 203(14) | 172(12) | 174(7) | 0.97(2) |
| P1 | 4 <i>e</i> | 0 | 0 | 0.4724(2) | 140(20) | $U_{_{11}}$ | 120(30) | 133(15) | 1.00(5) |
| P2 | 4 <i>e</i> | 0 | 0 | 0.9087(2) | 110(20) | U_{11} | 150(40) | 122(15) | 1.06(5) |
| 0 | 8 <i>g</i> | 0 | 1/2 | 0.8352(4) | 140(70) | 120(70) | 120(50) | 130(40) | 1.12(7) |
| Cl | 4 <i>e</i> | 0 | 0 | 0.2715(2) | 300(30) | $U_{_{11}}$ | 240(40) | 282(19) | 0.96(5) |

Table 3: Interatomic distances (pm) of La₂Cu₄P₄O₃ and La₅Cu₄P₄O₄Cl₃ within the first coordination spheres. Standard deviations are equal or smaller than 1 pm.

| La ₃ Cu ₄ P ₄ O ₂ | | | | | | | | | | | |
|---|----------------------|-----|-------|------|---|-----|-------|-----|---|-----|-------|
| La1: | 8 | P2 | 307.4 | Cu: | 2 | P1 | 235.7 | P1: | 4 | Cu | 235.7 |
| | 8 | Cu | 323.7 | | 2 | P2 | 245.4 | | 4 | La2 | 331.9 |
| | 2 | P1 | 374.6 | | 4 | Cu | 285.6 | P2: | 1 | P2 | 227.4 |
| La2: | 4 | 0 | 238.4 | | 2 | La1 | 323.7 | | 4 | Cu | 245.4 |
| | 4 | P1 | 331.9 | | 2 | La2 | 353.9 | | 4 | La1 | 307.4 |
| | 4 | Cu | 353.9 | | | | | 0: | 4 | La2 | 238.4 |
| | 4 | La2 | 381.8 | | | | | | | | |
| La ¿Cu ₄F | $La_5Cu_4P_4O_4Cl_2$ | | | | | | | | | | |
| La1: | 4 | 0 | 240.0 | La3: | 8 | P1 | 309.2 | P1: | 1 | P1 | 224.2 |
| | 4 | P2 | 335.2 | | 8 | Cu | 324.0 | | 4 | Cu | 247.2 |
| | 4 | Cu | 354.2 | Cu: | 2 | P2 | 235.7 | | 4 | La3 | 309.2 |
| | 4 | La2 | 378.2 | | 2 | P1 | 247.2 | P2: | 4 | Cu | 235.7 |
| | 1 | Cl | 385.2 | | 4 | Cu | 288.2 | | 4 | La1 | 335.2 |
| La2: | 4 | 0 | 235.5 | | 2 | La3 | 324.0 | 0: | 2 | La2 | 235.5 |
| | 1 | Cl | 314.8 | | 2 | La1 | 354.2 | | 2 | La1 | 240.0 |
| | 4 | Cl | 320.5 | | | | | Cl: | 1 | La2 | 314.8 |
| | 4 | La1 | 378.2 | | | | | | 4 | La2 | 320.5 |
| | | | | | | | | | | | |

90° pulse lengths of 2.5 µs and delays of 0.5 s. Phosphoric acid (85 %) was used as an external reference. All spectra were recorded with the Bruker Topspin software [16] and analyzed with the DMFIT software [17]. Chemical shifts are referenced to 85 % H, PO, solution. The experimental data are listed in Table 4.

3 Results and discussion

3.1 Crystal chemistry

The structures of La₂Cu₄P₄O₅ [12] and La₅Cu₄P₄O₄Cl₅ were refined from single crystal X-ray diffractometer data. Their unit cells are presented in Fig. 1. Large parts of both structures are similar, i.e. the [Cu₂P₂] anionic and the [LaO] cationic layers. A look at the interatomic distances (Table 3) shows almost similar values for these structural slabs. We

Table 4: ³¹P NMR parameters of La₂Cu₄P₄O₃: isotropic resonance shifts δ_{ico} (±1, in ppm); full width at half maximum (FWHM, ±0.01, in kHz), relative intensity $I_{\rm rel}$, degree of Gaussian (G) vs. Lorentzian (L) character of the central signal, spin-spin relaxation times T_2 (ms).

| Signal | $oldsymbol{\delta}_{iso}$ | FWHM | I _{rel} | G/L | T ₂ | |
|-----------------------------------|---------------------------|------|------------------|------|-----------------------|--|
| P ₂ ⁴⁻ (P2) | 459 | 17.7 | 1.00 | 0.12 | 0.61 | |
| P ³⁻ (P1) | 250 | 14.1 | 0.85 | 0.20 | 1.62 | |

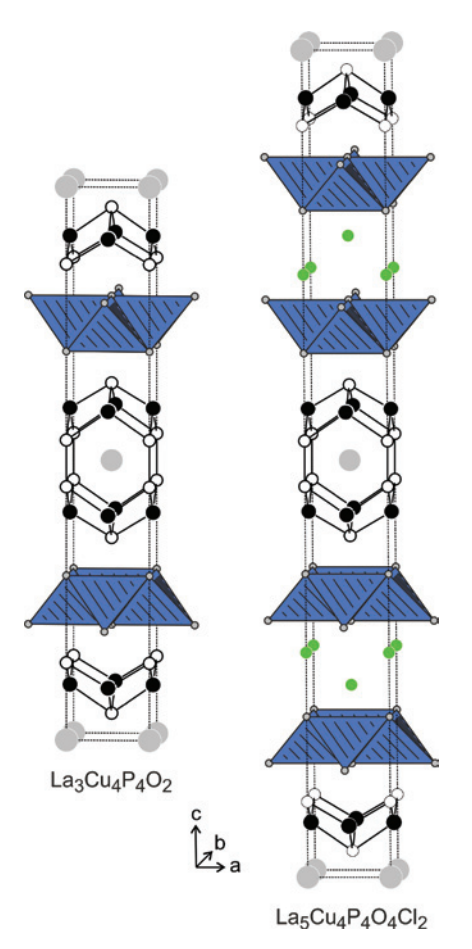


Fig. 1: The structures of La₃Cu₄P₄O₅ and La₅Cu₄P₄O₆Cl₅. Lanthanum, copper, phosphorus, and chlorine atoms are drawn as medium gray, black filled, black open, and green circles, respectively. The oxygen centered lanthanum tetrahedra and the polyanionic [CuP] networks are emphasized.

start the following crystal chemical discussion with the La₂Cu₄P₄O₅ structure.

La₂Cu₂P₄O₂ is the first member of a family of few quaternary phosphide oxides which are isopointal [18, 19] with the silicide Zr₃Cu₄Si₆ [20]. The rare earth (*RE*) compounds $RE_{2}Cu_{\mu}P_{\mu}O_{2}$ (RE = Ce, Pr, Nd, Sm) [12, 21] and $La_{2}Ni_{\mu}P_{\mu}O_{2}$ [22] are isotypic with $La_3Cu_\mu P_\mu O_3$. With the higher congener arsenic, the phases $RE_3T_4As_4O_{2-\delta}$ with RE = La, Ce, Pr, Nd, Sm, and T = Ni, Cu [10, 23] have recently been reported.

The main point regarding these phases contheir non-electron-precise description, e.g. $(3La^{3+})^{9+}(4Cu^+)^{4+}(P_2^{4-})(2P^{3-})^{6-}(2O^{2-})^{4-}$, leaving an excess negative charge. Partial oxygen occupancy of the oxygen sites, like in $Pr_3Cu_4P_4O_{1.50}$ and $Sm_3Cu_4P_4O_{1.63}$ [21] could be an explanation. Nevertheless, one has to keep in mind that La, Cu, P, O, is a metallic conductor and a black solid with metallic luster for crystalline pieces [12]. The original structure refinement of La₃Cu₄P₄O₅ showed an enhanced

isotropic displacement parameter for the oxygen site, which might be indicative of a split position or a reduced occupancy parameter. The present structure refinement allowed anisotropic refinement of all sites, and a separate refinement of the occupancy parameters gave no hint for oxygen vacancies. This is in line with the neutron powder diffraction data for La₃Ni₄P₄O₂ [22]. Oxygen vacancy formation was suggested for the arsenides $RE_{3}T_{4}As_{4}O_{2-8}$ [23], but not really substantiated on the basis of experimental data.

Assuming full occupancy of the oxygen site and the essentially ionic bonding between lanthanum and oxygen, the best approximation for an electron-precise formula splitting would be La³⁺(La₂O₂)²⁺(Cu₂P₂)⁵⁻, leaving the electronic adjustment to the pnictide polyanion. The latter has two degrees of freedom: (i) the P-P bond distance and (ii) the possibility of partial copper oxidation. While we observe a P–P distance of 227 pm in La₂Cu₄P₄O₃, close to the single bond distance of 223 pm [24], a much longer P-P distance of 258 pm occurs in La₃Ni₄P₄O₅ [22], a tendency towards breaking the P-P bond and leaving higher electron density at the phosphorus atoms as compared to La₃Cu₄P₄O₅.

This peculiar electronic situation is most likely directly related to the anisotropic coordination of the Cu₂P₂ layer: on one side by La³⁺ cations (higher cationic charge) and on the opposite side by the [LaO]+ layer (lower cationic charge). Especially for the series of RE_3T_4 As₄O₂₋₈ arsenides [23], this crystalline anisotropy strongly affects the magnetic and transport properties. In contrast, the pnictide layers of the many ZrCuSiAs phases [1] have isotropic coordination by [REO]+ layers on both sides (alternating AB stacking with the [TPn] layers).

The structural anisotropy discussed for La₂Cu₄P₄O₃ also occurs in the new quintenary compound La_sCu_n P_aO_aCl₂ which is isotypic with La_aCu_aAs_aO_aCl₂ [10]. The main difference to La₃Cu₄P₄O₂ concerns the insertion of two ionic LaOCl slabs in the unit cell. Similar to the quaternary compound, also for La_eCu_eP_eO_eCl_e the ionic formula splitting La³⁺(La₄O₄)⁴⁺(Cu₄P₄)⁵⁻(2Cl⁻)²⁻ is the best approximation. The electronic situation of the (Cu,P,)5slab is exactly the same in both compounds.

La_ECu_AP_AO_ACl_A is also a black compound and its metallic behavior is evident from the Pauli susceptibility (vide infra). Electronic structure calculations on isotypic La_eCu_e As, O, Cl, [10] led to a strongly anisotropic hybrid material with covalently bonded tetrahedral CuAs_{4/4} layers that are separated by larger ionic insulating oxide and chloride blocks. With respect to chemical bonding we can safely apply a rigid band model to La_sCu_aP_aO_aCl₃ described herein.

3.2 Magnetic properties of La_ECu_AP_AO_ACl_A

The temperature dependence of the magnetic susceptibility of La_cCu_aP_aO_aCl₃ is presented in Fig. 2. The overall

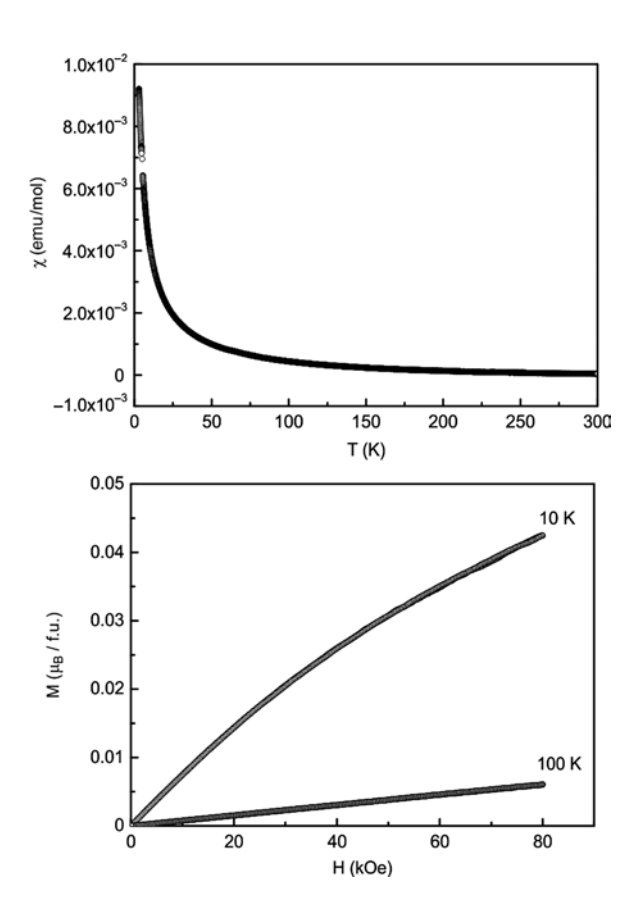


Fig. 2: Magnetic properties of La_eCu_eP_eO_eCl_e: (top) Temperature dependence of the magnetic susceptibility measured at 10 kOe; (bottom) Magnetization isotherms measured at 10 and 100 K.

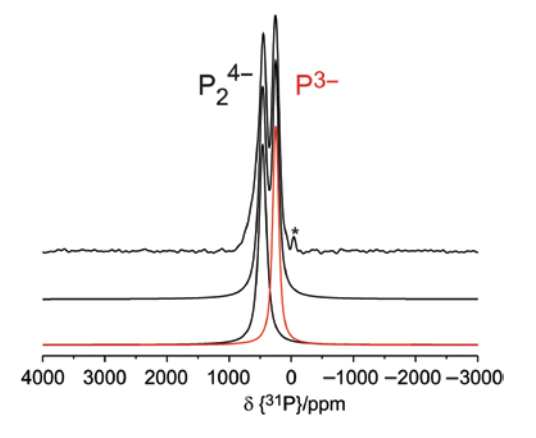


Fig. 3: 31P MAS NMR spectrum of La₃Cu₄P₆O₃ recorded at 28 kHz spinning frequency and its deconvolution into two distinct Gauss/ Lorentz components. The signal caused by an impurity is marked with an asterisk.

susceptibility data (Fig. 2, top) are low with a value of $\chi =$ $0.4(1) \times 10^{-4}$ emu mol⁻¹ at 300 K, classifying La₂Cu₂P₂O₂Cl₂ as a Pauli paramagnet. The upturn towards lower temperatures is due to a small paramagnetic contribution, most likely an impurity phase. In agreement with the low susceptibility data we also observe tiny moments in the magnetization isotherms at 10 and 100 K (Fig. 2, bottom). Low-field low-temperature measurements gave no hint for superconductivity.

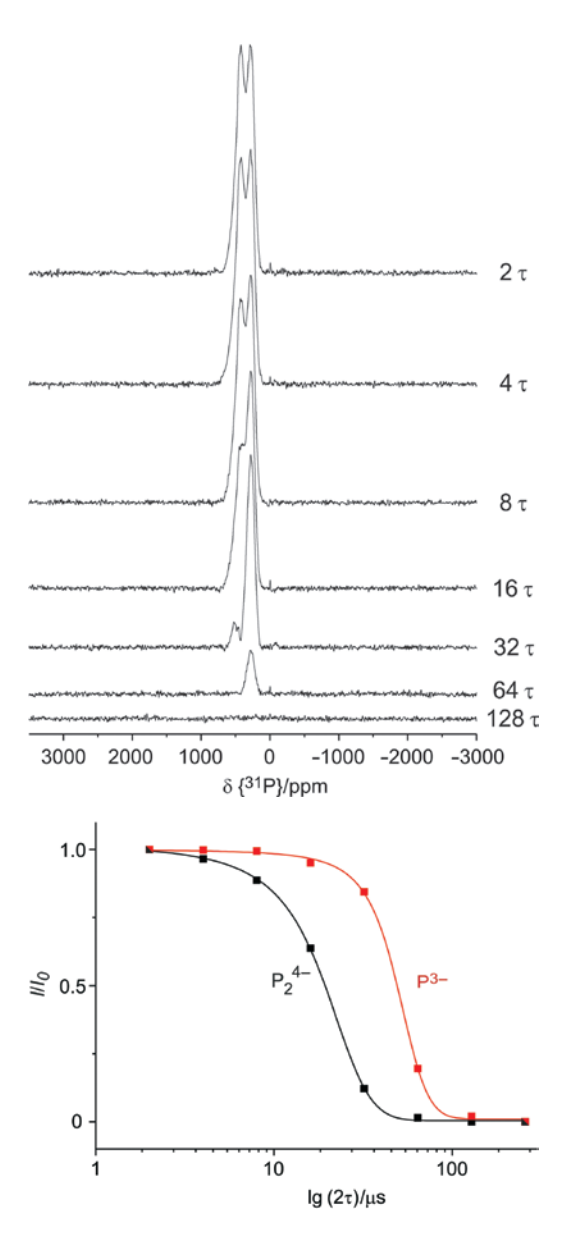


Fig. 4: $\pi/2 - \tau - \pi - \tau$ spin echo spectra of La₂Cu₂P₂O₃ recorded at 30 kHz spinning frequency with increasing evolution time $2\tau/\mu s$ (left) and intensity dependence of the signals on the effective evolution time (right). Solid curves represent the exponential decays corresponding to spin-spin relaxation times of 1.62 and 0.61 ms for P(1) and P(2), respectively.

3.3 ³¹P Solid state MAS NMR spectroscopic data of La₃Cu₄P₄O₅

The ³¹P MAS NMR spectrum of La₃Cu₄P₄O₂ is shown in Fig. 3. As expected, two signals are obtained, consistent with the two phosphorus sites of equal population (1:1 area ratio). The spin-lattice relaxation times are in the millisecond range, which is uncommonly short for spin-1/2 nuclei in the solid state. In addition, considerable resonance shifts relative to the H₃PO₄ standard are observed. These spectroscopic features are consistent with the metallic character previously reported for this compound from electrical conductivity and magnetic susceptibility measurements [12]. The large resonance shifts signify unpaired conduction electron spin density at the Fermi edge at the phosphorus sites, causing a Knight shift contribution to the resonance frequencies observed. For assigning the two distinct resonances at 250 and 459 ppm to the phosphorus sites P(1) and P(2) we can exploit the dependence of the homo-nuclear 31P-31P dipole-dipole interactions on the inter-nuclear distances. Owing to the direct P-P bond the P(2) species experience much stronger dipolar couplings than the isolated P(1) species. Experimentally, the dipolar coupling strength can be assessed by measuring the site-resolved spin-spin relaxation times T_2 by a rotor-synchronized $\pi/2 - \tau - \pi - \tau$ MAS-spin echo experiment with variable effective evolution times $2n \tau$ with $\tau =$ $v_{\rm rot}^{-1}$ (Fig. 4), where 2*n* is the number of rotor cycles. The results, summarized in Fig. 4 and Table 4, indicate that the spin-spin relaxation times of the two types of phosphorus species differ significantly and clearly suggest that the signal at 459 ppm must be assigned to the P₂⁴⁻ dumbbell species P(2).

Acknowledgments: This work was supported by the Deutsche Forschungsgemeinschaft. We thank Dr. Thomas Wiegand (ETH Zürich) for his participation in the early stages of this work.

References

- [1] R. Pöttgen, D. Johrendt, Z. Naturforsch. 2008, 63b, 1135.
- [2] T. C. Ozawa, S. M. Kauzlarich, Sci. Techn. Adv. Mater. 2008, 9,
- [3] D. C. Johnston, Adv. Phys. 2010, 59, 803.
- [4] D. Johrendt, H. Hosono, R.-D. Hoffmann, R. Pöttgen, Z. Kristallogr. 2011, 226, 435.
- [5] Z.-A. Ren, W. Lu, J. Yang, W. Yi, X.-L. Shen, Z.-C. Li, G.-C. Che, X.-L. Dong, L.-L. Sun, F. Zhou, Z.-X. Zhao, Chin. Phys. Lett. 2008, 25, 2215.

- [6] H. Kabbour, L. Cario, F. Boucher, J. Mater. Chem. 2005, 15, 3525
- [7] M. Tegel, S. Johansson, V. Weiss, I. Schellenberg, W. Hermes, R. Pöttgen, D. Johrendt, Eur. Phys. Lett. 2008, 84, 67007.
- [8] R. H. Liu, Y. A. Song, Q. J. Li, J. J. Ying, Y. J. Yan, Y. He, X. H. Chen, Chem. Mater. 2010, 22, 1503.
- [9] H. Kabbour, E. Janod, B. Corraze, M. Danot, C. Lee, M.-H. Whangbo, L. Cario, J. Am. Chem. Soc. 2008, 130, 8261.
- [10] M. Eul, D. Johrendt, R. Pöttgen, Z. Naturforsch. 2009, 64b, 1353.
- [11] D. E. Bugaris, H.-C. zur Loye, *Angew. Chem., Int. Ed.* **2012**, *51*, 3780.
- [12] R. J. Cava, H. W. Zandbergen, J. J. Krajewski, T. Siegrist, H. Y. Hwang, B. Batlogg, J. Solid State Chem. 1997, 129, 250.
- [13] K. Yvon, W. Jeitschko, E. Parthé, J. Appl. Crystallogr. 1977, 10, 73.
- [14] L. Palatinus, G. Chapuis, J. Appl. Crystallogr. 2007, 40, 786.
- [15] V. Petříček, M. Dušek, L. Palatinus, Z. Kristallogr. 2014, 229, 345.

- [16] Bruker Corp., Topspin (version 2.1), Karlsruhe, Germany,
- [17] D. Massiot, F. Fayon, M. Capron, I. King, S. Le Calvé, B. Alonso, J.-O. Durand, B. Bujoli, Z. Gan, G. Hoatson, *Magn. Reson. Chem.* 2002, 40, 70.
- [18] L. M. Gelato, E. Parthé, J. Appl. Crystallogr. 1987, 20, 139.
- [19] E. Parthé, L. M. Gelato, Acta Crystallogr. 1984, A40, 169.
- [20] F. Thirion, G. Venturini, B. Malaman, J. Steinmetz, B. Roques, J. Less-Common Met. 1983, 95, 47.
- [21] J. W. Kaiser, W. Jeitschko, Z. Naturforsch. 2002, 57b, 165.
- [22] T. Klimczuk, T. M. McQueen, A. J. Williams, Q. Huang, F. Ronning, E. D. Bauer, J. D. Thompson, M. A. Green, R. J. Cava, Phys. Rev. B 2009, 79, 012505.
- [23] J. K. Wang, A. Marcinkova, C.-W. Chen, H. He, M. Aronson, E. Morosan, *Phys. Rev. B* 2014, 89, 094405.
- [24] R. Pöttgen, W. Hönle, H. G. von Schnering, Phosphides: Solid State Chemistry, in Encyclopedia of Inorganic Chemistry, Vol. VII, 2nd ed. (Ed.: R. B. King), Wiley, New York, 2005, 4255.